

Scale-free localization versus Anderson localization in unidirectional quasiperiodic lattices

Yu Zhang,^{1,2} Luhong Su,³ and Shu Chen^{1,2,*}

¹*Beijing National Laboratory for Condensed Matter Physics,
Institute of Physics, Chinese Academy of Sciences, Beijing 100190, China*

²*School of Physical Sciences, University of Chinese Academy of Sciences, Beijing, 100049, China*

³*Department of Physics, The Hong Kong University of Science and Technology, Clear Water Bay, Kowloon, Hong Kong, China*

(Dated: February 21, 2025)

Scale-free localization emerging in non-Hermitian physics has recently garnered significant attention. In this work, we explore the interplay between scale-free localization and Anderson localization by investigating a unidirectional quasiperiodic model with generalized boundary conditions. We derive analytical expressions of Lyapunov exponent from the bulk equations. Together with the boundary equation, we can determine properties of eigenstates and spectrum and establish their exact relationships with the quasiperiodic potential strength and boundary parameter. While eigenstates exhibit scale-free localization in the weak disorder regime, they become localized in the strong disorder regime. The scale-free and Anderson localized states satisfy the boundary equation in distinct ways, leading to different localization properties and scaling behaviors. Generalizing our framework, we design a model with exact energy edges separating the scale-free and Anderson localized states via the mosaic modulation of quasiperiodic potentials. Our models can be realized experimentally in electric circuits.

Introduction. Non-Hermitian systems can exhibit some novel localization phenomena without Hermitian counterparts. A paradigmatic example is the non-Hermitian skin effect (NHSE), which manifests as the localization of majority of eigenstates at the boundary under open boundary conditions (OBC) [1–4]. NHSE is intrinsically related to non-Hermitian point gap [5–7] and highly sensitive to boundary conditions [8, 9]. The interplay between non-Hermiticity and disorder has created extreme richness to localization phenomena in generic non-Hermitian systems [10–13] and stimulated intensive studies on non-Hermitian systems with random disorder [13–21] or quasiperiodic disorder [22–50]. Competition between NHSE and Anderson Localization (AL) has been studied in Refs.[21, 26, 27], unveiling that the nonreciprocal hopping shifts the localization-delocalization transition point and induces a topological transition, where the rescaled transition point can be validated by the winding number [25, 26].

Recently, a distinctive type of non-Hermitian localization, coined as scale-free localization (SFL), has been proposed [51] and attracted intensive studies [52–66]. Unlike NHSE, where the localization length does not depend on the system size, SFL features a localization length proportional to the system size. It is striking that even a single non-Hermitian impurity in a Hermitian bulk lattice can generate a significant number of SFL modes [54], which challenges our conventional understanding of localization. The simplest model realizing SFL is the unidirectional hopping model [56, 57], which describes a system with hopping in only one direction. This model can be solved analytically [9] and is crucial for understanding the origin of SFL.

In this work, we investigate the interplay of SFL and

AL by considering the unidirectional hopping model with various quasiperiodical potentials. In unidirectional hopping lattices, due to the absence of reflection, one may wonder whether Anderson localized states can emerge, as usually the Anderson localization phenomenon arises from a destructive interference effect [67]. Although a recent work numerically demonstrated the existence of localized states in the unidirectional hopping lattice with random disorder [57], a theoretical understanding on the mechanism for the formation of localization and the transition between SFL and localized states is still lack.

Without loss of generality, we first consider the unidirectional quasiperiodic model as schematically shown in Fig.1(a), and demonstrate that the extension of the notation of Lyapunov exponent (LE) can describe either the localized state or SFL state. In the large size limit, we get analytical expressions for the LE. Combining with the boundary condition, we can determine both properties of eigenstates and spectrum, which allow us to study analytically the interplay between SFL and AL. A schematic phase diagram is provided in Fig.1(b). The scaling behavior of eigenvalues and eigenstates varies across different regions. In the weak disorder region, SFL persists but its properties are affected by disorder strength and boundary conditions. The SFL can be left-localized or right-localized depending on the value of boundary parameter. In contrast, the LE of localized state is determined by the bulk equation whereas the boundary equation gives the estimation of eigenvalues. Furthermore, we study the unidirectional quasiperiodic model with mosaic modulation and unveil the existence of SFL-AL edges.

Model and method. We consider a unidirectional chain with quasiperiodic potentials described by the following

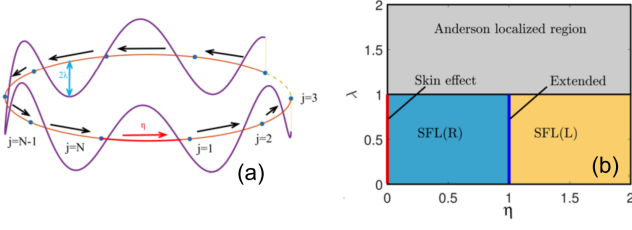


FIG. 1: (a) Schematic diagram of the unidirectional quasiperiodic model. (b) Schematic phase diagram of the unidirectional quasiperiodic model with different strength of quasiperiodic disorder (λ) and boundary hopping term (η).

Hamiltonian:

$$H = \sum_{j=1}^{L-1} t |j+1\rangle \langle j| + \eta |1\rangle \langle L| + \sum_{j=1}^L 2\lambda \cos(2\pi\alpha j) |j\rangle \langle j|, \quad (1)$$

where t represents the right hopping amplitude, $\alpha = \frac{\sqrt{5}-1}{2}$ is an irrational number and λ quantifies the strength of the quasiperiodic potential. The parameter η is the strength of the hopping term connecting the first and the last sites. Varying η can interpolate the OBC ($\eta = 0$) to periodic boundary condition (PBC) ($\eta = 1$). For arbitrary η , the boundary condition is referred to as a generalized boundary condition (GBC). For convenience, we adopt $t = 1$ as the unit of energy and set $\eta \geq 0$ throughout the following discussions.

In the absence of disorder, i.e., $\lambda = 0$, the model simplifies into the unidirectional hopping model with GBC and can be solved analytically [9, 56, 57]. The eigenvalues satisfy $E^L - \eta = 0$, resulting in an energy spectrum expressed as

$$E_m = \eta^{\frac{1}{L}} e^{i\theta_m}, \quad (\theta_m = \frac{2m\pi}{L}, m = 1, 2, \dots, L).$$

The eigenstates can be written as

$$|\psi_m\rangle = c_0 [1, \eta^{\frac{1}{L}} e^{i\theta_m}, \eta^{\frac{2}{L}} e^{i2\theta_m} \dots \eta^{\frac{L-1}{L}} e^{i(L-1)\theta_m}]^T,$$

where c_0 is the normalization factor. These eigenstates are localized at either the left or right edge with the localization length given by $\xi = L/|\ln(\eta)|$, which is proportional to the system size. The model can be regarded as a minimal model to realize SFL eigenstates.

In the presence of quasiperiodic potential, we can get the eigen equation in the bulk from Eq.(1), which reads as

$$Eu_j = u_{j-1} + 2\lambda \cos(2\pi\alpha j)u_j, \quad (2)$$

where u_j is the eigenstate distribution at the j -th site. It gives the following recursion relation:

$$u_j = \frac{1}{E - 2\lambda \cos(2\pi\alpha j)} u_{j-1}, \quad (3)$$

in which u_j only depends on u_{j-1} . To study the localization property of the eigenstate, we introduce the LE (γ) defined by

$$|u_{j+l_d}| \approx e^{-\gamma l_d} |u_j|, \quad (4)$$

where l_d is the distance between different sites. While $\gamma = 0$ indicates a delocalized eigenstate, $\gamma \neq 0$ indicates that the amplitude of the eigenstate decays ($\gamma > 0$) or grows ($\gamma < 0$) with the increasing distance. The localization length ξ is given by $\xi = 1/|\gamma|$.

Combining Eq.(3) and Eq.(4), we get the expression for the LE:

$$\gamma = \frac{1}{n} \sum_{j=1}^n \ln(|E - 2\lambda \cos[2\pi\alpha(j + j_0)]|),$$

where we assume the wavefunction starting from the j_0 -th site. Because of the non-monotonic nature of the cosine function, the single wavefunction does not decay strictly exponentially over short distance but exhibits exponential decay over long distance on average. If we consider a sufficiently long chain, we can make the transformation $2\pi\alpha(j + j_0) \rightarrow \theta$ and replace the sum with an integral [28, 35]. Then the LE can be expressed as

$$\gamma = \frac{1}{2\pi} \int_0^{2\pi} \ln(|E - 2\lambda \cos(\theta)|) d\theta. \quad (5)$$

The eigenvalues of a non-Hermitian system can be complex. Thus, we consider the LE in the entire complex plane:

$$\gamma = \begin{cases} \ln(|\lambda|) & \text{If } |E| \leq 2\lambda, \Im(E) = 0, \\ \ln \left| \frac{E + \sqrt{E^2 - (2\lambda)^2}}{2} \right| & \text{otherwise.} \end{cases} \quad (6)$$

It should be noted this function is a multi-valued function for complex E , and we have another restriction: $|\frac{E + \sqrt{E^2 - (2\lambda)^2}}{2\lambda}| > 1$, which can also be written as $\gamma > \ln(|\lambda|)$. The details of the calculation can be found in the supplement material [68].

Further, considering the GBC, we obtain the boundary equation which connects the eigenstate distribution at the first site to the last site:

$$u_1 = \frac{\eta}{E - 2\lambda \cos(2\pi\alpha 1)} u_L.$$

Using the recursion relation Eq.(3) iteratively $L-1$ times, we get a self-consistent equation:

$$\eta \prod_{j=1}^L \frac{1}{E - 2\lambda \cos(2\pi\alpha j)} = 1. \quad (7)$$

Using Eq.(7) and Eq.(6), we can determine both the distribution of eigenvalues and the properties of the eigenstates. We shall show that there exist two different mechanisms to fulfill Eqs.(7) and (6) simultaneously in the SFL and AL regimes, respectively.

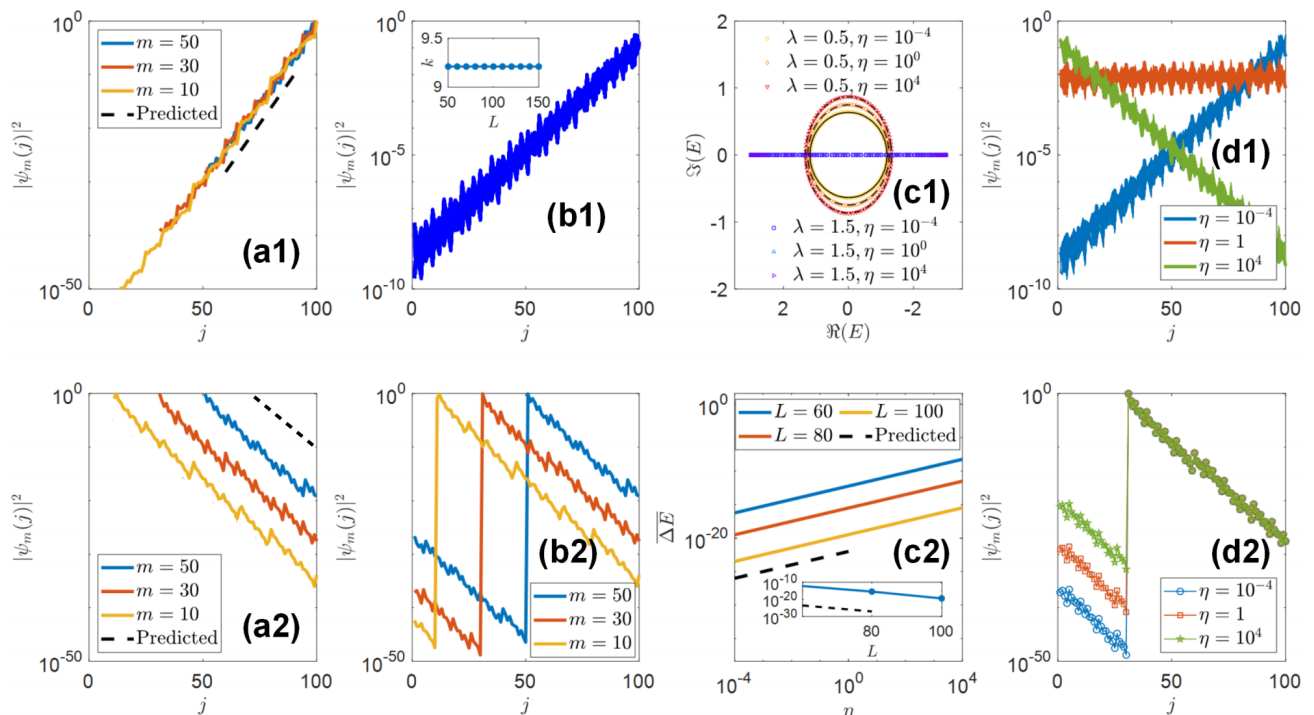


FIG. 2: Eigenvalues and eigenstates for the unidirectional quasiperiodic model with different boundary conditions. (a1-a2) Typical eigenstates for different disorder strengths under OBC: $\lambda = 0.5$ (a1) and $\lambda = 1.5$ (a2). The dashed line represents the decay of the wave function predicted by theoretical analysis. (b1-b2) Eigenstates for systems under GBC with $\eta = 10^{-4}$: all eigenstates with $\lambda = 0.5$ (b1) and typical eigenstates with $\lambda = 1.5$ (b2). We apply a linear fitting procedure to $\ln(|\psi|)$ and j/L : $\ln(|\psi|) = k(j - j_0)/L + c$. The inset in (b1) shows how the slope varies with system size. (c1) Spectrum for the system with various λ and η . The points are the eigenvalues from ED and the black lines are the analytical results. The black solid line, dashed line, and dash-dotted line correspond to $\eta = 10^{-4}$, $\eta = 1$, and $\eta = 10^4$, respectively. (c2) $\Delta\bar{E}$ versus η for system with $\lambda = 1.5$ and different L . The inset shows $\Delta\bar{E}$ versus L . Both dashed black lines have the slopes predicted by our analytical results and are consistent with the results from ED. (d1) All eigenstates in the region of $\lambda = 0.5$ with different boundary parameters. We choose $L = 100$. (d2) Some typical eigenstates in the region of $\lambda = 1.5$ with different boundary parameters. We choose $m = 30$ and $L = 100$.

Interplay of SFL and localization. We first consider the case under the OBC, which gives a boundary equation $Eu_1 = 2\lambda \cos(2\pi\alpha)u_1$. It is shown that $E = 2\lambda \cos(2\pi\alpha)$ is an eigenvalue of the system with the wavefunction of the eigenstate determined by using Eq.(3) iteratively. From the Eq.(2), we see

$$E_m = 2\lambda \cos(2\pi\alpha m), \quad m = 1 \dots L$$

are eigenvalues of the system. The eigenstate corresponding to E_m is confined to the region $[m, L]$ with $u_i = 0$ for all $i < m$ and other u_j with $j = m, \dots, L$ determined by using Eq.(3) iteratively. In Fig.2 (a1) and (a2), we display distributions of wavefunctions for several typical eigenstates in the region of $|\lambda| < 1$ and $|\lambda| > 1$, respectively. For $|\lambda| < 1$, all the eigenstates accumulate at the right boundary and terminate at the site m with the LE $\gamma < 0$, indicating that these eigenstates are skin states. For $|\lambda| > 1$, the distribution of eigenstate decays exponentially in a unidirectional way from the m th site towards the right boundary. These states are localized states with localized centers at the m th site. Localization

properties of both skin states and localized eigenstates can be characterized by the LE given by $\gamma = \ln(|\lambda|)$. A transition from NHSE to AL occurs at $|\lambda| = 1$. Although the eigenvalues are given by a uniform formula $E_m = 2\lambda \cos(2\pi\alpha m)$ for any λ , the behavior of eigenstates are quite different for $|\lambda| < 1$ or $|\lambda| > 1$.

Now we consider the case under the GBC. In the region of $\lambda < 1$, for example $\lambda = 0.5$, all eigenstates are localized at the right edge, as displayed in Fig.2(b1). From the finite size analysis, we find that the localization length is proportional to the system size L , as shown in the inset of Fig.2(b1). This can be understood from the self-consistent equation (7). Using the definition of the LE, Eq.(7) can be alternatively represented as $\eta e^{-L\gamma} = 1$, which gives

$$\gamma = \frac{\ln(\eta)}{L}. \quad (8)$$

It indicates that γ is inversely proportional to system size L . In other words, the localization length is proportional to the system size, and the eigenstates are SFL.

In this region, the eigenvalues are complex as shown in Fig.2(c1). In the large size limit, the complex eigenvalues can be analytically determined by $\gamma = \ln \left| \frac{E + \sqrt{E^2 - (2\lambda)^2}}{2} \right|$, which gives rise to

$$\frac{E_r^2}{[1 + (2\lambda)^2/(4e^{2\gamma})]^2} + \frac{E_i^2}{[1 - (2\lambda)^2/(4e^{2\gamma})]^2} = e^{2\gamma} \quad (9)$$

as long as $\ln(|\lambda|) < \frac{\ln(\eta)}{L}$, where $e^\gamma = \eta^{\frac{1}{L}}$. Eq.(9) suggests that the complex spectrum forms an ellipse. The numerical results presented in Fig.2(c1) verify the spectrum distribution predicted by Eq.(9). The effect of the boundary parameter η to eigenstates is shown in Fig.2(d1). By varying the strength of η , we observe the transition from ‘left SFL’ to extended states and ‘right SFL’. The sign of γ is determined by $\ln(\eta)$ and $\eta = 1$ is the transition point between the left SFL and right SFL.

In the region of $\lambda > 1$, for example $\lambda = 1.5$, the eigenstates are localized states which decay exponentially in a unidirectional way, as shown in Fig.2(b2). For a given λ , all eigenstates have the same LE $\gamma = \ln(|\lambda|)$. Due to the existence of boundary terms, the distribution of eigenstate u_i in the region $i < m$ is no longer zero and keeps exponential decay in a unidirectional way. While the eigenstate distributes continuously at the boundary for $\eta = 1$, the eigenstates exhibit a sharp decrease and increase at the boundary for $\eta = 10^{-4}$ and $\eta = 10^4$, respectively, as shown in Fig.2(d2).

In Fig.2(c1), we present the energy spectrum for $\lambda = 1.5$ and various η . All eigenvalues are distributed along the real axis and are very close to each other. Although the eigenvalues of localized states are not sensitive to the boundary condition, the eigenvalues are no longer given by $2\lambda \cos(2\pi\alpha m)$ in the presence of the boundary term ($\eta \neq 0$). Deviation from the on-site potential can be estimated by Eq.(7), which can be simplified as:

$$\Delta E_m = E_m - 2\lambda \cos(2\pi\alpha m) \approx e^{\ln(\eta) - \ln(|\lambda|)(L-1)}. \quad (10)$$

By using this equation, we can estimate the dependence of ΔE_m on η and the scaling behavior of ΔE_m . In Fig.2(c2), we show $\overline{\Delta E}$ versus η for different L , where $\overline{\Delta E} = \frac{1}{L} \sum_{m=1}^L \Delta E_m$. The scaling behavior got from numerical results are consistent with our analytical analysis. Eq.(10) holds true as long as $\ln(|\lambda|) > \frac{\ln(\eta)}{L}$. The details about the analytical discussion can be found in the supplementary material [68].

Our results unveil that SFL states manifest when $|\lambda| < \eta^{1/L}$, whereas the system enters the AL region when $|\lambda| > \eta^{1/L}$. The SFL-localization transition accompanies with a transition from complex to real spectrum. We note that the transition point $|\lambda_c| = \eta^{1/L}$ is size dependent. For a given η , when $L \rightarrow \infty$, $\eta^{1/L} \rightarrow 1$.

SFL-AL edges in the mosaic model. Next we consider a unidirectional mosaic quasiperiodic model with

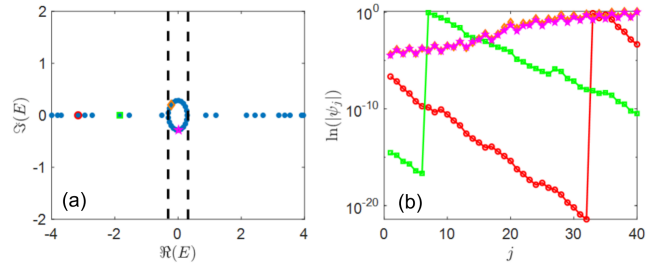


FIG. 3: (a) Eigenvalues for the unidirectional mosaic quasiperiodic model with GBC. The dashed lines indicate the predicted SFL-AL edges. (b) Distributions of typical eigenstates for the unidirectional mosaic quasiperiodic model. The curves of different colors and markers correspond to the eigenvalues of the corresponding colors and markers in (a). Here we choose $\lambda = 2$, $\eta = 10^{-4}$, $\kappa = 2$ and $L = 40$.

the Hamiltonian given by:

$$H_\kappa = \sum_{j=1}^{\kappa L-1} t|j+1\rangle\langle j| + \eta|1\rangle\langle \kappa L| + \sum_{j=1}^{\kappa L} \lambda_j|j\rangle\langle j|, \quad (11)$$

where $\lambda_j = 2\lambda \cos(2\pi\alpha j)$, if $\text{mod}(j, \kappa) = 0$ and $\lambda_j = 0$ otherwise. By using iteration relations, we can find that the distribution of eigenstates at different sites fulfills:

$$u_{j+\kappa-1} = \frac{1}{E^{\kappa-1}[E - 2\lambda \cos(2\pi\alpha j)]} u_{j-1}.$$

From the bulk equation, we can get the expression of the LE:

$$\gamma = \begin{cases} \ln(|\lambda|) + (\kappa - 1) \ln(|E|), & \text{if } |E| \leq 2\lambda, \Im(E) = 0 \\ \ln \left| \frac{E + \sqrt{E^2 - (2\lambda)^2}}{2} \right| + (\kappa - 1) \ln(|E|), & \text{Others.} \end{cases}$$

Considering the boundary condition, we can derive the SFL-AL edge given by:

$$\Re(E) = \pm \frac{\eta^{\kappa/L(\kappa-1)}}{|\lambda|^{1/(\kappa-1)}}. \quad (12)$$

All eigenstates with $|\Re(E)| < \frac{\eta^{\kappa/L(\kappa-1)}}{|\lambda|^{1/(\kappa-1)}}$ are SFL states and eigenstates with $|\Re(E)| > \frac{\eta^{\kappa/L(\kappa-1)}}{|\lambda|^{1/(\kappa-1)}}$ are localized[68]. Here the SFL-AL edge is size dependent. Different from the Hermitian case, the multiple mobility edges emerging in the Hermitian mosaic model with $\kappa \geq 3$ [69] disappear in the unidirectional model. In Fig.3(a), we present the results from the exact diagonalization and the exact SFL-AL edge predicted by our method. In Fig.3(b), we show some typical eigenstates which exhibit SFL or AL behavior. For $\eta = 1$, the mobility edge is given by $\Re(E) = \pm |\lambda|^{-1/(\kappa-1)}$, which separates the extended states from the localized states.

Summary and discussion. We studied the effect of quasiperiodic potentials in a unidirectional hopping lattice with GBC. By calculating the LE analytically, we

explored the interplay between SFL and AL and identified the transition point from SFL to AL is given by $\eta^{1/L}$. In different phase regions, two types of eigenstates satisfy the boundary condition through different mechanisms. The SFL eigenstates are characterized by the localization length $\xi = L/|\ln(\eta)|$ and acquire complex eigenvalues which distribute on an ellipse. In contrast, the localized eigenstates are characterized by the localization length $\xi = \ln|\lambda|$ and have real eigenvalues which align closely with the on-site potentials. Further generalizing our framework, we designed a model with accurate SFL-AL edges via the mosaic modulation of quasiperiodic potentials. Our theoretical scheme can be directly extended to study other unidirectional quasiperiodic systems.

Our analytical results establish exact relationships between parameters (η and λ) and behaviors of the system. Our study unveils the important role of the boundary term in the formation of SFL and the estimation of spectrum properties of localized states, deepening our understanding of the underlying mechanisms of transition between SFL and AL. We can also design electric circuits to simulate our models [68], which helps us generalize the theory to practical applications.

We thank Qi Zhou and Mingchen Zheng for useful discussions. This work is supported by National Key Research and Development Program of China (Grant No. 2023YFA1406704) and the NSFC under Grants No.12474287 and No. T2121001.

* Electronic address: schen@iphy.ac.cn

- [1] S. Yao and Z. Wang, Edge states and topological invariants of non-hermitian systems, *Phys. Rev. Lett.* **121**, 086803 (2018).
- [2] F. K. Kunst, E. Edvardsson, J. C. Budich and E. J. Bergholtz, Biorthogonal bulk-boundary correspondence in non-Hermitian systems, *Phys. Rev. Lett.* **121**, 026808 (2018).
- [3] V. M. Martinez Alvarez, J. E. B. Vargas, and L. E. F. F. Torres, Non-Hermitian robust edge states in one dimension: Anomalous localization and eigenspace condensation at exceptional points, *Phys. Rev. B* **97**, 121401(R) (2018).
- [4] K. Yokomizo and S. Murakami, Non-Bloch Band Theory of Non-Hermitian Systems, *Phys. Rev. Lett.* **123**, 066404 (2019).
- [5] N. Okuma, K. Kawabata, K. Shiozaki and M. Sato, Topological origin of non-hermitian skin effect, *Phys. Rev. Lett.* **124**, 086801 (2020).
- [6] K. Zhang, Z. Yang and C. Fang, Correspondence between winding numbers and skin modes in non-hermitian systems, *Phys. Rev. Lett.* **125**, 126402 (2020).
- [7] D. S. Borgnia, A. J. Kruchkov, and R.-J. Slager, Non-Hermitian Boundary Modes and Topology, *Phys. Rev. Lett.* **124**, 056802 (2020).
- [8] C. H. Lee and R. Thomale, Anatomy of skin modes and topology in non-Hermitian systems, *Phys. Rev. B* **99**, 201103 (2019).
- [9] C.-X. Guo, C.-H. Liu, X.-M. Zhao, Y. Liu, and S. Chen, Exact Solution of Non-Hermitian Systems with Generalized Boundary Conditions: Size-Dependent Boundary Effect and Fragility of the Skin Effect, *Phys. Rev. Lett.* **127**, 116801 (2021).
- [10] D. Bernard and A. LeClair, A classification of non-Hermitian random matrices, *Stat. Field Theor.* **73**, 207 (2002).
- [11] L. G. Molinari, Non-Hermitian spectra and Anderson localization, *Journal of Physics A: Mathematical and Theoretical* **42**, 265204 (2009).
- [12] X. Luo, T. Ohtsuki, and R. Shindou, Universality classes of the Anderson transitions driven by non-Hermitian disorder, *Phys. Rev. Lett.* **126**, 090402 (2021).
- [13] K. Kawabata and S. Ryu, Nonunitary scaling theory of non-Hermitian localization, *Phys. Rev. Lett.* **126**, 166801 (2021).
- [14] N. Hatano and D. R. Nelson, Localization transitions in non-hermitian quantum mechanics, *Phys. Rev. Lett.* **77**, 570 (1996).
- [15] N. Hatano and D. R. Nelson, Non-hermitian delocalization and eigenfunctions, *Phys. Rev. B* **58**, 8384 (1998).
- [16] N. M. Shnerb and D. R. Nelson, Winding Numbers, Complex Currents, and Non-Hermitian Localization, *Phys. Rev. Lett.* **80**, 5172 (1998).
- [17] J. Feinberg and A. Zee, Non-hermitian localization and delocalization, *Phys. Rev. E* **59**, 6433 (1999).
- [18] A. V. Kolesnikov and K. B. Efetov, Localization-delocalization transition in non-hermitian disordered systems, *Phys. Rev. Lett.* **84**, 5600 (2000).
- [19] Y. Huang and B. I. Shklovskii, Spectral rigidity of non-Hermitian symmetric random matrices near the Anderson transition, *Phys. Rev. B* **102**, 064212 (2020).
- [20] Cem Yuce and Hamidreza Ramezani, Coexistence of extended and localized states in the one-dimensional non-Hermitian Anderson model, *Phys. Rev. B* **106**, 024202 (2022).
- [21] J. Claes and T. L. Hughes, Skin effect and winding number in disordered non-hermitian systems, *Phys. Rev. B* **103**, L140201 (2021).
- [22] A. Avila, Global theory of one-frequency Schrödinger operators, *Acta. Math.* **1**, 215, (2015).
- [23] Y. Wang, X. Xia, J. You, Z. Zheng, and Q. Zhou, Exact mobility edges for 1D quasiperiodic models, *Commun. Math. Phys.* **401**, 2521 (2023).
- [24] A. Jazaeri and I. I. Satija, Localization transition in incommensurate non-Hermitian systems, *Phys. Rev. E* **63**, 036222 (2001).
- [25] S. Longhi, Topological phase transition in non-hermitian quasicrystals, *Phys. Rev. Lett.* **122**, 237601 (2019).
- [26] H. Jiang, L. J. Lang, C. Yang, S. L. Zhu, and S. Chen, Interplay of non-hermitian skin effects and anderson localization in nonreciprocal quasiperiodic lattices, *Phys. Rev. B* **100**, 054301 (2019).
- [27] Y. Liu, Q. Zhou, and S. Chen, Localization transition, spectrum structure, and winding numbers for one-dimensional non-Hermitian quasicrystals, *Phys. Rev. B* **104**, 024201 (2021).
- [28] S. Longhi, Metal-insulator phase transition in a non-hermitian aubry-andré-harper model, *Phys. Rev. B* **100**, 125157 (2019).
- [29] Q. B. Zeng, Y. B. Yang, and Y. Xu, Topological phases

- in non-hermitian aubry-andré-harper models, *Phys. Rev. B* **101**, 020201 (2020).
- [30] Y. Liu, X.-P. Jiang, J. Cao, and S. Chen, Non-Hermitian mobility edges in one-dimensional quasicrystals with parity-time symmetry, *Phys. Rev. B* **101**, 174205 (2020).
- [31] Q.-B. Zeng and Y. Xu, Winding numbers and generalized mobility edges in non-Hermitian systems, *Phys. Rev. Research* **2**, 033052 (2020).
- [32] T. Liu, H. Guo, Y. Pu, and S. Longhi, Generalized Aubry-Andre self-duality and mobility edges in non-Hermitian quasiperiodic lattices, *Phys. Rev. B* **102**, 024205 (2020).
- [33] Y. Liu, Y. Wang, X.-J. Liu, Q. Zhou, and S. Chen, Exact mobility edges, PT-symmetry breaking and skin effect in one-dimensional non-Hermitian quasicrystals, *Phys. Rev. B* **103**, 014203 (2021).
- [34] X. Cai, Boundary-dependent Self-dualities, Winding Numbers and Asymmetrical Localization in non-Hermitian Quasicrystals, *Phys. Rev. B* **103**, 014201 (2021).
- [35] S. Longhi, Phase transitions in a non-Hermitian Aubry-Andre-Harper model, *Phys. Rev. B* **103**, 054203 (2021).
- [36] L.-J. Zhai, S. Yin, G.-Y. Huang, Many-body localization in a non-Hermitian quasi-periodic system, *Phys. Rev. B* **102**, 064206 (2020).
- [37] Y. Liu, Y. Wang, Z. Zheng, S. Chen, Exact non-Hermitian mobility edges in one-dimensional quasicrystal lattice with exponentially decaying hopping and its dual lattice, *Phys. Rev. B* **103**, 134208 (2021).
- [38] X. Cai, Anderson localization and topological phase transitions in non-Hermitian Aubry-Andre-Harper models with p-wave pairing, *Phys. Rev. B* **103**, 214202 (2021).
- [39] Z. Xu, X. Xia, and S. Chen, Non-Hermitian Aubry-Andre model with power-law hopping, *Phys. Rev. B* **104**, 224204 (2021).
- [40] L.-Z. Tang, G.-Q. Zhang, L.-F. Zhang, and D.-W. Zhang, Localization and topological transitions in non-Hermitian quasiperiodic lattices, *Phys. Rev. A* **103**, 033325 (2021).
- [41] Q. Lin, T. Li, L. Xiao, K. Wang, W. Yi, and P. Xue, Topological Phase Transitions and Mobility Edges in Non-Hermitian Quasicrystals, *Phys. Rev. Lett.* **129**, 113601 (2022).
- [42] W. Han and L. Zhou, Dimerization-induced mobility edges and multiple reentrant localization transitions in non-Hermitian quasicrystals, *Phys. Rev. B* **105**, 054204 (2022).
- [43] L. Zhou, Non-Abelian generalization of non-Hermitian quasicrystals: PT-symmetry breaking, localization, entanglement, and topological transitions, *Phys. Rev. B* **108**, 014202 (2023).
- [44] W. Chen, S. Cheng, J. Lin, R. Asgari, and G. Xianlong, Breakdown of the correspondence between the real-complex and delocalization-localization transitions in non-Hermitian quasicrystals, *Phys. Rev. B* **106**, 144208 (2022).
- [45] T. Liu and X. Xia, Real-complex transition driven by quasiperiodicity: A class of non-PT symmetric models, *Phys. Rev. B* **105**, 054201 (2022).
- [46] S. Gandhi and J. N. Bandyopadhyay, Topological triple phase transition in non-Hermitian quasicrystals with complex asymmetric hopping, *Phys. Rev. B* **108**, 014204 (2023).
- [47] A. Padhan, S. R. Padhi, and T. Mishra, Complete de-localization and reentrant topological transition in a non-Hermitian quasiperiodic lattice, *Phys. Rev. B* **109**, L020203 (2024).
- [48] S.-Z. Li and Z. Li, Ring structure in the complex plane: A fingerprint of a non-Hermitian mobility edge, *Phys. Rev. B* **110**, L041102 (2024).
- [49] L. Wang, Z. Wang, and S. Chen, Non-Hermitian butterfly spectra in a family of quasiperiodic lattices, *Phys. Rev. B* **110**, L060201 (2024).
- [50] A. P. Acharya and S. Datta, Localization transitions in a non-Hermitian quasiperiodic lattice, *Phys. Rev. B* **109**, 024203 (2024).
- [51] L. Li, C. H. Lee and J. Gong, Impurity induced scale-free localization, *Commun. Phys.* **4**, 42 (2021).
- [52] L. Li, C. H. Lee, S. Mu, and J. Gong, Critical non-Hermitian skin effect, *Nat. Commun.* **11**, 5491 (2020).
- [53] K. Yokomizo and S. Murakami, Scaling rule for the critical non-Hermitian skin effect, *Phys. Rev. B*, **104**, 165117 (2021).
- [54] C. Guo, X. Wang, H. Hu and S. Chen, Accumulation of scale-free localized states induced by local non-Hermiticity, *Phys. Rev. B* **107**, 134121 (2023).
- [55] B. Li, H. Wang, F. Song and Z. Wang, Scale-free localization and PT symmetry breaking from local non-Hermiticity, *Phys. Rev. B* **108**, L161409 (2023).
- [56] L. Su, C. Guo, Y. Liang, L. Li, X. Ruan, Y. Du, S. Chen and D. Zheng, Observation of size-dependent boundary effects in non-Hermitian electric circuits, *Chin. Phys. B* **32**, 038401 (2023).
- [57] P. Mognini, S. Arandes and E. J. Bergholtz, Anomalous skin effects in disordered systems with a single non-hermitian impurity, *Phys. Rev. Research* **5**, 033058 (2023).
- [58] H.-R. Wang, B. Li, F. Song, and Z. Wang, Scale-free non-Hermitian skin effect in a boundary-dissipated spin chain, *SciPost Phys.* **15**, 191 (2023).
- [59] Y. Fu and Y. Zhang, Hybrid scale-free skin effect in non-Hermitian systems: A transfer matrix approach, *Phys. Rev. B* **108**, 205423 (2023).
- [60] X. Xie, G. Liang, F. Ma, Y. Du, Y. Peng, E. Li, H. Chen, L. Li, F. Gao, and H. Xue, Observation of scale-free localized states induced by non-Hermitian defects, *Phys. Rev. B* **109**, L140102 (2024).
- [61] B. Yilmaz, C. Yuce, and C. Bulutay, From scale-free to Anderson localization: A size-dependent transition, *Phys. Rev. B* **110**, 214206 (2024).
- [62] C.-X. Guo, L. Su, Y. Wang, L., J. Wang, X. Ruan, Y. Du, D. Zheng, S. Chen and H. Hu, Scale-tailored localization and its observation in non-Hermitian electrical circuits, *Nat Commun* **15**, 9120 (2024).
- [63] W. Li, Z. Sun, Z. Yang, and F. Li, Universal scalefree non-Hermitian skin effect near the Bloch point, *Phys. Rev. B* **109**, 035119 (2024).
- [64] G.-J. Liu, J.-M. Zhang, S.-Z. Li, and Z. Li, Emergent strength-dependent scale-free mobility edge in a nonreciprocal long-range Aubry-Andre-Harper model, *Phys. Rev. A* **110**, 012222 (2024).
- [65] J. Zhang, K.-X. Hu, C.-L. Zhang, X.-F. Nie, Z.-X. Zhang, Y. Yan, J. Cao, S. Zhang, and H.-F. Wang, PT-symmetric phase transition and unidirectional accumulation of eigenstates in a non-Hermitian system with a single impurity, *Phys. Rev. A* **110**, 062216 (2024).
- [66] H. Spring, V. Könye, A. R. Akhmerov, I. C. Fulga, Lack of near-sightedness principle in non-Hermitian systems,

- SciPost Phys. **17**, 153 (2024).
- [67] P. W. Anderson, Absence of Diffusion in Certain Random Lattices, Phys. Rev. **109**, 1492 (1958).
- [68] See Supplemental Material for (I). Details for the calculation of LE. (II). Discussions on eigenvalues and eigenstates of the unidirectional quasiperiodic model. (III). Boundary sensitivity in GBC. (IV). LE of unidirectional mosaic quasiperiodic model. (V). Realization in classical electric circuits.
- [69] Y. C. Wang, X. Xia, L. Zhang, H. P. Yao, S. Chen, J. G. You, Q. Zhou, and X. J. Liu, One-dimensional quasiperiodic mosaic lattice with exact mobility edges, Phys. Rev. Lett. **125**, 196604 (2020).